Hydrogen Impurity Effects. A_5Tt_3Z Intermetallic Compounds between A = Ca, Sr, Ba, Eu, Yb and Tt = Sn, Pb with Cr_5B_3-like Structures That Are Stabilized by Hydride or Fluoride (Z)

E. Alejandro Leon-Escamilla and John D. Corbett*

Department of Chemistry and Ames Laboratory−DOE,[1] Iowa State University, Ames, Iowa 50011

Received September 13, 2000

The binary systems Ca−Sn, Ba−Sn, Eu−Sn, Yb−Sn, Sr−Pb, Ba−Pb, and Eu−Pb do not contain Cr_5B_3-like A_5Tt_3 phases when care is taken to exclude hydrogen from the reactions (Tt = tetrel, Si−Pb). All form ternary $A_5Tt_3H_x$ phases ($x \leq 1$) with "stuffed" Cr_5B_3-like structures instead, and all of those tested, Ca−Sn, Ba−Sn, Sr−Pb, and Ba−Pb, also yield the isostructural A_5Tt_3F. The structures and compositions of $Ca_5Sn_3H_x$, $Ca_5Sn_3F_{0.89}$, $Eu_5Sn_3H_x$, and Sr_5Pb_3F have been refined from single-crystal X-ray diffraction data and of Ca_5Sn_3D from powder neutron data. The interstitial H, F atoms are bound in a tetrahedral $(A^{2+})_4$ cavity in a Cr_5B_3-type metal atom structure. Nine previous reports of binary "Ba_5Sn_3", "Yb_5Sn_3", "Sr_5Pb_3", and "Ba_5Pb_3" compounds were wrong and presumably concerned the hydrides. The new ternary phases are generally Pauli-paramagnetic, evidently with π^* electrons from the characteristic tetrelide dimers in this structure type at least partially delocalized into the conduction band. The Sn−Sn bonds appear correspondingly shortened on oxidation. Other new phases reported are CaSn (CrB type), $Yb_5Sn_4H_x$ (Sm_5Ge_4), YbSn (∼TlTe), Ba_5Pb_3 (∼W_5Si_3), and $Yb_{31}Pb_{20}$ ($Ca_{31}Sn_{20}$).

Introduction

Compounds formed between alkali, alkaline-earth, or rare-earth metals and the main group p elements have been major features in the development of some diverse structural and bonding aspects of solid-state chemistry. The main-group components most often feature the tetrels (Si family, Tt), pnictogens (P family principally), and chalcogens. One common feature of many of these products is the predominance of valence or closed-shell compounds, the so-called Zintl phases.[2] On the other hand, the earlier triel (Al family) members afford classical closed-shell anions less often and instead feature more hypoelectronic or metallic (electron-rich) examples.[3] Contradictions or inconsistencies between our results and those in the literature, or, equally often, an inability to obtain a reported compound in high yield, have repeatedly forced us into a consideration of phase stabilization via unrecognized impurities. Carbon, nitrogen, and oxygen are naturally common candidates, but hydrogen has turned out to be a particularly pervasive problem both because its presence has usually not been considered and because of the fact that the atom is essentially undetected in heavy atom compounds by common X-ray diffraction methods for phase detection or analysis.

The first systematic exploration stemmed from our inability to sort out the formation of Mn_5Si_3- from β-Yb_5Sb_3-type pnictides of the alkaline-earth and dipositive rare-earth metals. The problem was solved with the discovery that all nine examples of the latter-assigned structure type were in fact valence hydrides $(A^{II})_5Pn_3H$[4,5] in the orthorhombic Ca_5Sb_3F structure type.[6] This was the first instance in our work in which fluoride was utilized as a good stand-in for hydride and which is easily located by modern X-ray diffraction means, although this relationship has been known for much longer.[7] The most prevalent sources of hydrogen impurities have been commercial alkaline-earth metals, although most active metals can become so contaminated with careless handling. (Hydrogen is usually retained on their reactions with adventitious water.) Examples in the same Mn_5Si_3-type systems in which the pnictide hydride forms first, or only, by utilizing a well-characterized interstitial hole[8] in that structure type will be described in a forthcoming manuscript.[9] Other specific hydride errors have included the Zintl phases $Ba_5Ga_6H_2$ [10] and $Ba_{21}M_2O_5H_{22+x}$ (M = Si, Ge, Ga, etc.; $x = 2, 0$),[11] the structures of which were originally reported without the hydrogen components.

Similar events have shadowed the chemistry of the related A_5Tt_3 phases of the tetrel (Tt) elements Si−Pb. These are frequently encountered in a tetragonal Cr_5B_3-type structure with its characteristic equal numbers of monomeric and dimeric anions, meaning that those with divalent cations formally meet the structural criterion for Zintl phases,[12] $(A^{2+})_5(Tt_2^{6-})(Tt^{4-})$ in terms of oxidation states. One might even anticipate that these closed-shell configurations should be immune to oxidation and thence to the inclusion of hydride without a necessary change

(1) This research was supported by the Office of the Basic Energy Sciences, Materials Sciences Division, U.S. Department of Energy. The Ames Laboratory is operated for DOE by Iowa State University under Contract W-7405-Eng-82.

(2) Kauzlarich, S., Ed. *Chemistry, Structure, and Bonding of Zintl Phases and Ions*; VCH Publishers: Boca Raton, FL, 1996.
(3) Corbett, J. D. *Angew. Chem., Int. Ed. Engl.* **2000**, *39*, 670.
(4) Leon-Escamilla, E. A.; Corbett, J. D. *J. Alloys Compd.* **1994**, *206*, L15.
(5) Leon-Escamilla, E. A.; Corbett, J. D. *J. Alloys Compd.* **1998**, *265*, 104.
(6) Hurng, W.-M.; Corbett, J. D. *Chem. Mater.* **1989**, *1*, 311.
(7) Messer, C. E. *J. Solid State Chem.* **1970**, *2*, 144.
(8) Corbett, J. D.; Garcia, E.; Guloy, A. M.; Hurng, W.-M.; Kwon, Y.-U.; Leon-Escamilla, E. A. *Chem. Mater.* **1998**, *10*, 2824.
(9) Leon-Escamilla, E. A.; Corbett, J. D. Manuscript to be published.
(10) Henning, R. W.; Leon-Escamilla, E. A.; Zhao, J.-T.; Corbett, J. D. *Inorg. Chem.* **1997**, *36*, 1282.
(11) Huang, B.; Corbett, J. D. *Inorg. Chem.* **1998**, *37*, 1892.
(12) Hughbanks, T. In *Inorganometallic Chemistry*; Fehlner, T., Ed.; Plenum Press: New York, 1992; p 291.

10.1021/ic0010306 CCC: $20.00
Published on Web 02/06/2001

of structure type. In fact, the problems here are particularly insidious because not only is oxidation of the substrate by hydrogen generally possible but the hydride formed is also readily incorporated into a suitable cavity already present in the parent Cr_5B_3 structure. This article will be limited to the seven instances in which only an example of a stuffed Cr_5B_3 structure is stable in the new Ca_5Sn_3F structure type (or the hydride equivalent). These hydride errors have been the source of nine erroneous reports of binary tetragonal $A_5(Tt)_3$ tetrelide phases. In these cases, either the truly binary A_5Tt_3 compositions occur in another structure type or the composition yields only a mixture of other binary phases. More complicated instances in which both the binary and the ternary (hydride) systems occur with the same heavy atom Cr_5B_3 structure type will be described in a later article.[13] The latter occurrence of parallel stabilities naturally means that X-ray lattice constant values are probably the quickest and best way to tell them apart, and these are usually the only means available in retrospection, although comparison of dimensional data from different time periods and equipment naturally entails some problems. It should be noted that still six others in this family of A_5Tt_3 compounds, apparently only for Sm and Yb, form hydrides with a stuffed Mn_5Si_3H-type structure instead, another future topic.[13]

The presence of a significant tetrahedral cavity in the Cr_5B_3 structure type was first signaled by the serendipitous discovery of a stuffed Cr_5B_3-type structure for La_5Pb_3O (via a sample of dirty lead).[14] In the presence of these electron-richer cations, the lead atoms (Pb^{4-} nominally) are now all monomeric, without a dimer, and the analogous nitride would appear to be electron-precise. (A similar disposition of monoanions is also known in the so-called In_5Bi_3 subfamily.[15])

What evolved into a broad examination of these Cr_5B_3-type triels started with a negative situation, the fact that the composition Ca_5Sn_3 had never been reported, in considerable contrast to the rest of the family. In the course of this search, we instead discovered that a novel alternative, the oligomeric $Ca_{31}Sn_{20}$, was stable at a close-lying composition, 60.8 atom % Ca vs 62.5 atom % for Ca_5Sn_3,[16] and on the basis of earlier experience, we went on to show that only $Ca_5Sn_3H_x$ and Ca_5Sn_3F form in a now-stuffed Cr_5B_3-type structure. We choose to distinguish the structure of La_5Pb_3O and the absence of a dimer from the situation in the new Ca_5Sn_3F structure type where the dimeric anion is retained, although both types occur in the same space group and are isopointal.

The protocol developed earlier for studies of the Mn_5Si_3H vs Ca_5Sb_3F-type phases[5] was again used to test for the formation of hydride derivatives as well as to ensure the absence of impurity hydrogen in checks for the formation of true Cr_5B_3 types and other binary phases. Although it is possible to clean the alkaline-earth metals, etc. beforehand by careful dissociation of hydrogen in a vacuum, it is generally far easier to simply load the components in tantalum tubing, weld this shut, and heat the assembly in high vacuum at, say, 900−1200 °C. The metals and any hydride compounds will have appreciable H_2 dissociation pressures under these conditions, and tantalum is permeable to only hydrogen in our systems above 550−600 °C. Subsequent equilibrations in a virtually hydrogen-free system can then be made at suitable temperatures. On the other hand, sample containers loaded with hydrogen sources, e.g., CaH_2, are equilibrated in Ta only after their further enclosure in sealed silica jackets to retain the hydrogen. Some additional hydrogen can still form in smaller amounts from water dissociation from the fused silica over longer periods and at higher temperatures. (This may also be signaled by an oxide impurity in the products but not always.) These two routes will hereafter be designated as dynamic vacuum (dv) and sealed (SiO_2) container (sc).

Experimental Section

Materials utilized were Ca, Sr, Ba (Ae) from APL Engineering, distilled and sealed in glass; Sm, Eu, and Yb, Ames Laboratory, ≥99.95% total; Sn and Pb, Aesar 5−9's or better. The AH_2 phases were prepared by direct reaction of H_2 with the metals in a Mo boat in a closed vacuum system equipped with a diaphragm manometer. Reactions were run to completion at 420−700 °C under 600−700 Torr H_2, the conditions being selected according to dissociation characteristics of the particular hydrides.[17] All were treated as stoichiometric AH_2 phases except for hexagonal $SmH_{\geq 2.5}$, as verified by their cell dimensions.[17,18] The AeF_2 reagents were precipitated from $AeCO_3$ slurries with excess HF(aq), filtered, washed, and vacuum-dried at 400 °C.

In particular cases, the as-received alkaline-earth metals and Yb were dehydrogenated after sealing them in Ta containers. These were heated in silica tubing under high vacuum ($\leq 10^{-5}$ Torr), namely, at 650 °C for Ca and at 710 °C for the remainder for ∼12 h or until the vacuum fell below that producing a Tesla coil discharge after a small increase in temperature.

All reactions between the elements with or without fluorides or hydrides were carried out in welded Ta containers that were heated either under vacuum or within evacuated, well-flamed, and sealed silica jackets. All reagents and products were handled in gloveboxes with 0.2−0.4 ppm (vol) H_2O levels. These techniques as well as those for Guinier powder pattern measurements (with NIST Si as an internal standard) and subsequent lattice constant least-squares refinement methods have been described in more detail before.[5,19,20] A Cu Kα1 wavelength of 1.540 56 Å was used for the last. The phase distributions in products were estimated in terms of equivalent X-ray scattering powers from their patterns with the aid of calculated patterns for known phases. Although the accuracies of these estimates vary perhaps by ±2−5%, they are internally more precise than that. All phases seen are reported.

Single crystals for X-ray diffraction were selected under low magnification and mounted in thin-walled glass capillaries in a glovebox for four of the phases reported here. These were first checked for quality through Laue photographs. Later tables detail data collection and refinement parameters. Absorption was corrected for with the aid of three ψ scans collected at $\chi \geq 80°$, and after isotropic refinement, with DIFABS. Structural refinements were made with the TEXSAN[21] package. Lattice dimensions secured from Guinier powder pattern data calibrated with Si were used in all distance calculations from single-crystal results. The anisotropic displacement parameters are available in the Supporting Information. These and the F_o/F_c listings are also available from J.D.C. Neutron diffraction data were collected on the high-resolution powder diffractometer HB-4 at Oak Ridge National Laboratory at room temperature.[22] Approximately 3.0 g of powdered sample prepared as $Ca_5Sn_3D_x$ was sealed in an In-gasketed V can. Data were collected over $11 \leq 2\theta \leq 135°$ over ca. 20 h.

(13) Leon-Escamilla, E. A.; Corbett, J. D. *J. Solid State Chem.*, submitted.
(14) Guloy, A. M.; Corbett, J. D. *Z. Anorg. Allg. Chem.* **1992**, *616*, 61.
(15) Böttcher, P.; Doert, Th.; Druska, Ch.; Bradtmöller, S. *J. Alloys Compd.* **1997**, *246*, 209.
(16) Ganguli, A. K.; Guloy, A. M.; Leon-Escamilla, E. A.; Corbett, J. D. *Inorg. Chem.* **1993**, *32*, 4349.
(17) Magee, C. B. In *Metal Hydrides*; Mueller, W. M., Backledge, J. P., Libowitz, G. G., Eds.; Academic Press: New York, 1968; Chapter 6.
(18) Villars, P.; Calvert, L. D. *Pearson's Handbook of Crystallographic Data for Intermetallic Phases*, 2nd ed.; American Society for Metals International: Metals Park, OH, 1991.
(19) Guloy, A. M.; Corbett, J. D. *Inorg. Chem.* **1993**, *32*, 3532.
(20) Leon-Escamilla, E. A.; Hurng, W.-M.; Peterson, E. S.; Corbett, J. D. *Inorg. Chem.* **1997**, *36*, 703.
(21) *TEXSAN, Single Crystal Structure Analysis Software*, version 5.0; Molecular Structure Corp.: The Woodlands, TX, 1989.
(22) Dervenagas, P.; Leon-Escamilla, E. A.; Stassis, C.; Corbett, J. D. Unpublished research.

Table 1. Stuffed Cr_5B_3-Type Phases Stabilized by Interstitial H or F

		approximate yield, %[b]			Cr_5B_3-type lattice dimensions[c]			
loaded composition/ref	conditions[a]	C	CB	other	*a*, Å	*b*, Å	*V*, Å^3	*a*/*c*
Ca_5Sn_3	dv 1	0	5	90P, ox				
$Ca_5Sn_3H_{0.0}$	sc 1	0	10	85P, ox				
$Ca_5Sn_3H_{1.0}$	sc 1	65	5	25P, ox	8.1433(6)	15.096(4)	1001.1(3)	0.539
$Ca_5Sn_3H_{2.0}$	sc 1	95	5		8.1472(3)	15.093(2)	1001.9(1)	0.540
Ca_5Sn_3F	dv 2	>95	<5		8.1331(4)	15.175(2)	1003.8(1)	0.536
$Ca_5Sn_3D_x$	fg 3	95	5		8.1450(3)	15.073(1)	999.97(9)	0.540
Ba_5Sn_3	dv 1	0		65CS, ~30CB, ox				
$Ba_5Sn_3H_{2.0}$	sc 1	80	20	ox	8.9491(5)	17.037(3)	1364.4(2)	0.525
Ba_5Sn_3F	dv 1	80	15	$5BaF_2$	8.9470(5)	17.014(3)	1361.9(2)	0.526
ref 26					9.02(1)	16.78(2)	1365(3)	0.537
ref 27					8.959	16.941	1359.7	0.529
Eu_5Sn_3	sc 4	0		90WS, un				
$Eu_5Sn_3H_{2.0}$	sc 1	90	5	un	8.4645(3)	15.589(1)	1116.9(1)	0.543
Yb_5Sn_3	dv 1	0		95YS, 5NI				
$Yb_5Sn_3H_{2.0}$	sc 5	10		85YS	8.080(1)	14.682(3)	958.5(3)	0.550
$Yb_5Sn_4D_{4.0}$	sc 1	15		80SG, 5GC	8.0952(4)	14.695(1)	963.0(1)	0.550
ref 28					7.939	14.686	925.6	0.540
Sr_5Pb_3	dv 1			95P				
$Sr_5Pb_3H_{2.0}$	sc 1	95	5		8.6674(5)	15.932(1)	1196.7(1)	0.544
Sr_5Pb_3F	dv 1	>95	<5		8.6679(5)	15.958(2)	1196.2(2)	0.542
ref 27					8.67	15.94	1198	0.544
ref 29					8.680(2)	15.935(8)	1200.6(9)	0.545
Ba_5Pb_3	dv 1	0		>95WS, ox	(14.148(2)	6.4288(9)	1286.8(3)	$(0.454)^{-1}$)
$Ba_5Pb_3H_{2.0}$	sc 1	15		80WS, ox	9.076(13)	16.524(25)	1361(3)	0.549
Ba_5Pb_3F	dv 1	20		70WS, $5BaF_2$	9.0538(5)	16.845(1)	1380.8(2)	0.537
ref 30					9.04(1)	16.943(7)	1376(2)	0.537
ref 31					9.040	16.816	1364.2	0.538
ref 29					9.055(1)	16.757(4)	1374.1(4)	0.540
Eu_5Pb_3	dv 1	0		100WS				
$Eu_5Pb_3H_{2.0}$	sc 1	30		70WS	~8.58[d]	−16.35[d]	1204	

[a] Conditions: dv = dynamic vacuum; sc = sealed silica jacket; fg = flowing D_2. 1: ~1150 °C for 6−8 h, 10 °C/h to 650 °C, cool in furnace. 2: 1200 °C for 6 h, 1100 °C for 8 h, 10 °C/h to 650 °C. 3: 1000 °C dv for 1 h, under D_2 at 1200 °C for 6 h, cool to 850 °C at 5 °C/h, hold 3d, to 650 °C at 10 °C/h. 4: As for condition 1 but annealed 34 d at 810 °C. 5: 1150 °C for 2 h, 5 °C/h to 900 °C, 3d, quenched. [b] Structural types: C−Cr_5B_3, P−$Pu_{31}Pt_{20}$, CB−CrB (orthorhombic), CS−Co_2Si, YS−$Yb_{36}Sn_{23}$, NI−Ni_2In, SG−Sm_5Ge_4, GC−AuCu, WS−W_5Si_3. ox: cubic Ca_3TtO. un: unknown. [c] Lattice dimensions from Guinier powder patterns with Si as internal standard, 23 °C. [d] Semiquantitative.

Magnetic susceptibility data were secured from weighed samples held between two fused silica rods that fit smugly inside a 5 mm o.d. tube in an apparatus sealed under He. The measurements were made with the aid of a Quantum Design MPMS superconducting quantum interference device (SQUID) magnetometer at 3 T and between 6 and 300 K. The data were corrected for the susceptibilities of both the apparatus and the atomic cores in the sample. Band structure calculations for Ca_5Sn_3H were performed at 45 k-points using the extended Hückel tight-bonding approximation.[23] The atom parameters H_{ii} (eV) and ζ (from Alvarez[24]) were the following: Ca 4s, −7.00, 1.10; Ca 4p, −4.00, 1.10; Sn 5s, −16.16, 2.12; Sn 5p, −8.32, 1.82; H 1s, −13.60, 1.30.

Results and Discussion

With hindsight, the case for hydrogen as a common impurity in the more active metal components and therefore possibly in their compounds is compelling, even obvious. These metals generally react with traces of water either at room temperature (for the more active) or at elevated temperatures with retention of the hydrogen as hydride, and ordinary vacuum sublimation or distillation of the alkaline-earth metals (Ca, Sr, Ba) mainly separates them from the oxide unless a prior dehydrogenation is done with some care. But it remains poorly appreciated that most of these available commercially have over the years contained noteworthy amounts of hydrogen, 5−20 atom % H over the group being reported in 1987,[25] and therefore that intermetallic or other studies with these sources may result in the formation of unrecognized ternary or higher hydrides. The seven tin and lead systems reported here, Ca−Sn, Ba−Sn, Eu−Sn, Yb−Sn, Sr−Pb, Ba−Pb, Eu−Pb, all form stuffed Cr_5B_3-type structures or, better, Ca_5Sn_3H-type hydrides and, where tested, the Ca_5Sn_3F isotypes as well. The additional binding of H^- or F^- thus tips the scale of stability, whereas all of the corresponding A_5Tt_3 binary compositions exhibit other structures or, in one case, only a mixture of other phases. Four of these have been misreported to form Cr_5B_3-type binary phases: Ba_5Sn_3,[26,27] Yb_5Sn_3,[28] Sr_5Pb_3,[27,29] and Ba_5Pb_3.[29−31]

None of the Cr_5B_3-like phases reported here exhibits a distortion to a primitive tetragonal cell known as the Ba_5Si_3 type. The weak extra lines indicative of this can be distinguished in good quality Guinier films if one knows what to look for.[13]

Table 1 contains a selection of the experimental reactions, results, and lattice constants that support these conclusions. The first, Ca−Sn, received the most extensive investigations. The Ca_5Sn_3 composition that reacted under dv (dynamic vacuum) conditions produces mainly the $Ca_{31}Sn_{20}$ [16] phase. When this was run neat with as-received materials but in a sealed system

(23) Whangbo, M. H.; Hoffmann, R.; Woodward, R. B. *Proc. R. Soc. London* **1978**, *100*, 3686.
(24) Alvarez, A. Tables of Parameters of Extended Hückel Calculations, Parts 1 and 2, Barcelona, Spain, 1987.
(25) Peterson, D. T. *J. Met.* **1987**, *39*, 20.
(26) Dorrscheidt, W.; Widera, A.; Schäfer, H. *Z. Naturforsch.* **1977**, *32B*, 1097.
(27) Bruzzone, G.; Franceschi, E.; Merlo, F. *J. Less-Common Met.* **1978**, *60*, 59.
(28) Palenzona, A. Cirafici, S. *J. Less-Common Met.* **1976**, *46*, 321.
(29) Druska, Ch. Ph.D. Dissertation, Heinrich Heine University, Düsseldorf, Germany, 1995.
(30) Sands, D. E.; Wood, D. H.; Ramsey, W. J. *Acta Crystallogr.* **1964**, *17*, 986.
(31) Bruzzone, G.; Franceschi, E. *J. Less-Common Met.* **1977**, *52*, 211.

(sc) instead, reaching as high as 1150 °C in the process, small amounts of the contaminant cubic Ca_3SnO (inverse perovskite[32]), presumably from water evolved from the silica, and the new calcium-poorer orthorhombic CaSn (CrB type[18]) from the stoichiometry upset were also seen. Five $Ca_5Sn_3H_y$ reactions incrementing hydrogen over $0.25 \le y \le 2.0$ (sc) produced regularly decreasing amounts of $Ca_{31}Sn_{20}$ and increasing amounts of $Ca_5Sn_3H_x$, from 20% of the latter at $y = 0.25$ to >95% for $y = 2.0$ (We do not know the H_2 dissociation characteristics of this new phase at 650 °C, the final equilibration temperature, but the reduced yields are consistent with some loss.) A 0.11% (3.0σ) increase in the hydride cell volumes over this range is very marginal evidence for a nonstoichiometry. Otherwise, the regular increases in yields of a dimensionally fixed hydride with increased hydrogen content are quite consistent with expectations for a product of nearly fixed composition that precipitates after some minimum activity of hydride and $P(H_2)$ are reached. Synthesis of the analogous fluoride from the composition Ca_5Sn_3F (dv) was achieved in high yield. Additionally, variations of the reaction stoichiometry over $Ca_5Sn_{3.0\pm0.3}$ (dv) produced nothing unusual; a $Ca_5SnF_{1.5}$ composition also yielded CaF_2 along with the requisite CaSn, and the stoichiometry $Ca_5Sn_3O_{0.5}$ gave ~70% $Ca_{31}Sn_{20}$, ~25% CaSn, and cubic Ca_3SnO.

Combined X-ray and neutron diffraction studies of the hydride (deuteride) yielded a refined composition of $Ca_{5.0}Sn_{3.00}H_{\sim1.0}$ and, for the fluoride (X-ray only), $Ca_{5.00}Sn_{3.00}F_{0.89(1)}$ with occupancy of the same tetrahedral site by H or F (details later).

Other Stannides. The compound Ba_5Sn_3 does not exist, at least at 650 °C or above, such a composition yielding ~65% Ba_2Sn (Co_2Si type[18]) and ~30% BaSn (CrB), while $Ba_5Sn_3H_{2.0}$ (sc) and Ba_5Sn_3F (dv) yield ~80% of the corresponding tetragonal A_5B_3Z phases plus principally BaSn. Clearly the two reports of "Ba_5Sn_3"[26,27] must have pertained to the hydride, although the dimensional differences from our results, particularly in *c* and one *V*, suggest some range of hydrogen content may have been present, especially in this case in which there is no nearby phase in competition. On the other hand, there is always an uncertainty as to how accurate the reported 1977 and 1978 lattice dimensions were.

The existence of the $Eu_5Sn_3H_x$ phase is clear (Table 1), and its X-ray structure has been refined (below). The absence of hydrogen affords the W_5Si_3-like Eu_5Sn_3, although we were able to obtain a powder pattern in good agreement with that calculated for the structure reported by Palenzona et al.[33] only for a sample that had been slowly cooled from 1100 °C (Table 1, condition 1) but annealed at 810 °C for several weeks. Samples treated in the more usual way gave related but clearly different patterns with both missing and extra lines and could not be accounted for by the neighboring phases in the binary system. We were not able to align a single crystal from the product on the diffractometer with a tetragonal W_5Si_3-like cell either. There must be one or more additional structures involved in this system. These may relate to a serious problem associated with the refinement of W_5Si_3-type structures, at least for compounds in this region,[33,34] including Ba_5Pb_3 below. These all show a substantial disorder (or misplacement) of the cation bound in the string of Sn, Pb, etc. tetrahedra that run along $\vec{c}$. In the present case, their refinement of this Eu atom gave an extreme U_{33}:U_{11} ratio of about 22:1.[33] Clearly this must represent only an approximation to some "real" structure.

On the other hand, a Yb_5Sn_3 composition gives primarily the recently reported $Yb_{36}Sn_{23}$[35] (plus a little Yb_2In, Ni_2In type), while two hydride (deuteride) reactions (Table 1) yielded 10−15% of $Yb_5Sn_3H_x$ plus either $Yb_{36}Sn_{23}$ at 900 °C or, with more hydrogen and at 650 °C, Yb_5Sn_4 (Sm_5Ge_4 type). (The latter suggested some hydride chemistry is involved for Yb_5Sn_4, and this has subsequently been confirmed by Yb_5Sn_4 reactions with and without hydrogen. The former gave the $Yb_5Sn_4H_x$ (Sm_5Ge_4 type), and the latter gave principally the new YbSn (TlTe type, $a = 12.4602(5)$ Å, $c = 6.0810(5)$ Å). These synthesis conditions are not optimal; $Yb_{36}Sn_{23}$ and $Yb_5Sn_4H_x$ must be relatively competitive with $Yb_5Sn_3H_x$ at 900 and 650 °C, respectively. More details will appear later.[9])

The earlier report of a Cr_5B_3-type "Yb_5Sn_3" presumably originated from a hydride impurity as did their "Yb_5Sn_4" as well.[28] However, the distinctly smaller volume reported for the former must mean either that they had substantially more bound hydride, the usual trend when [H] is a variable,[5,13] or that there was an appreciable error in the *a* dimension. Their phase diagrams also exhibit some complications. The Cr_5B_3-like version was always found mixed with another phase, which was only tentatively assigned as a Mn_5Si_3 type because of an uncertain fit of the powder pattern. The latter was probably $Yb_{36}Sn_{23}$ instead, and its comixture with "Yb_5Sn_3" is reasonable because the two phases would not have the same composition. But the assignment of a 1090 °C thermal effect to a transition between the two supposed Yb_5Sn_3 polytypes, with the Cr_5B_3 type being stable at higher temperature, is now left open and may pertain to other synthetic problems. The peritectic decomposition at 1235 °C assigned to the Cr_5B_3-type phase probably applies to $Yb_{36}Sn_{23}$. (They later noted that the Yb used had not been very pure.[36])

Plumbides. The known $Sr_{31}Pb_{20}$ ($Pu_{31}Pt_{20}$ [16]) is the stable product near a 5:3 composition, whereas $Sr_5Pb_3H_{2.0}$ and Sr_5Pb_3F compositions each yielded ~95% of the tetragonal Sr_5Pb_3(H,F) (Ca_5Sn_3F type). Two earlier claims of only tetragonal "Sr_5Pb_3" in this system must have again originated with substantial hydrogen impurities. Another recent report of this supposed compound indicated that it was a component of the ternary Sr−Pb−O system, without any details.[37] The structure of the fluoride has been refined (below).

The Ba_5Pb_3 composition was found to afford a new example of the well-known tetragonal W_5Si_3-type structure (for which the lattice dimensions are given in Table 1 in parentheses), whereas inclusion of hydrogen or fluorine gave 15−20% of the Ca_5Sn_3F-type Ba_5Pb_3Z. This hydride product was particularly reactive, and we were not able to obtain good lattice constant data, although the phase was clearly evident in the powder pattern. The syntheses achieved are again not optimal perhaps because of the lack of sufficient excess H_2. The Cr_5B_3-type binary compound that has been reported three times[29−31] in this system was presumably the hydride, and the hydrogen contamination in two cases[29,31] must have been severe enough to preclude recognition of the W_5Si_3-type Ba_5Pb_3. (Our attempts to refine the tetragonal "W_5Si_3" structure of Ba_5Pb_3 were incomplete because of the evidently generic disorder of the W_5Si_3 structure type as described above for Eu_5Sn_3.)

The Eu_5Pb_3 results are similar; the known W_5Si_3 type is formed for the binary and the analogous $Eu_5Pb_3H_x$ (Ca_5Sn_3F

(32) Widera, A.; Schäfer, H. *Mater. Res. Bull.* **1980**, *15*, 1805.
(33) Palenzona, P.; Manfrinetti, P.; Fornasini, M. L. *J. Alloys Compd.* **1998**, *280*, 211.
(34) Ganguli, A. K.; Leon-Escamilla, E. A.; Corbett, J. D. Unpublished research.
(35) Leon-Escamilla, E. A.; Corbett, J. D. *Inorg. Chem.* **1999**, *38*, 738.
(36) Palenzona, A.; Cirafici, S. *J. Phase Equilib.* **1991**, *12*, 482.
(37) Jacob, K. T.; Jayadevan, K. P. *Chem. Mater*. **2000**, *12*, 1781.

Table 2. Some Crystallographic Data for Refined X-ray Structures

	$Ca_5Sn_3H_x$	$Ca_5Sn_3F_{0.89(1)}$	$Eu_5Sn_3H_x$	Sr_5Pb_3F
fw	557.47	575.47	1116.87	1078.67
space group, Z		*I*4/*mcm* (No. 140), 4		
density calcd (g/cm^3)[a]	3.703	3.807	6.635	5.975
abs coeff (cm^{-1})	98.8	98.8	342.3	636.7
R_{ave}[b] (%)	3.32	2.99	11.1	16.0
R/R_w[c] (%)	1.7/1.9	1.4/1.5	3.5/4.3	4.6/5.1

[a] Lattice parameters obtained from Guinier powder patterns, Table 1. [b] All data $I > 0$. [c] $R = \sum||F_o| - |F_c||/\sum|F_o|$; $R_w = [\sum w(|F_o| - |F_c|)^2/\sum w(F_o)^2]^{1/2}$; $w = \sigma_F^{-2}$.

Table 3. Refined Positional (and Displacement) Parameters for $Ca_5Sn_3(H,F)_x$ Phases (X-ray Data) and for Ca_5Sn_3D and CaSn (Neutron Data)

atom[a]	*x*	*y*	*z*	B_{eq} (Å^2)[b]	10^2U_{iso} [c]
		$Ca_5Sn_3(H_x)$			
Ca1	0	0	0	1.81(4)	
Ca2	0.16254(7)	$x + 1/2$	0.15156(6)	1.31(2)	
Sn1	0	0	1/4	1.22(1)	
Sn2	0.37401(4)	$x + 1/2$	0	1.07(1)	
(H	0	1/2	1/4)		
		$Ca_5Sn_3F_{0.9}$			
Ca1	0	0	0	1.62(4)	
Ca2	0.16222(6)	$x + 1/2$	0.15082(4)	1.21(1)	
Sn1	0	0	1/4	0.97(1)	
Sn2	0.37401(4)	$x + 1/2$	0	0.801(8)	
F[d]	0	1/2	?	0.2(1)	
		Ca_5Sn_3D			
Ca1	0	0	0		2.3(1)
Ca2	0.1605(2)	$x + 1/2$	0.1521(2)		1.25(7)
Sn1	0	0	1/4		0.9(1)
Sn2	0.3749(2)	$x + 1/2$	0		0.40(7)
D	0	1/2	1/4		2.2(1)
		CaSn (CrB type)			
Ca1	0	0.1334(9)	1/4		2.1(3)
Sn2	0	0.4157(7)	1/4		0.8(2)

[a] Wyckoff designations for Ca1, Ca2, Sn1, Sn2, and Z (H or F) atom positions are 4*c*, 16*l*, 4*a*, 8*h*, and 4*b*, and the site symmetries are 4/*m*, ...*m*, 422, *m*.2*m*, and 42*m*, respectively. [b] $B_{eq} = (8\pi^2/3)\sum_i\sum_j U_{ij}a_i^*a_j^*\bar{a}_i\bar{a}_j$. [c] $T = \exp(-8\pi^2U_{iso}\sin^2(\theta/\lambda^2))$. [d] Occupancy was refined to 0.89(1).

type) with hydrogen, the conditions used in the survey yielding only ~30% of the latter and poor-quality powder patterns. Evidently the W_5Si_3 forms of Ba_5Pb_3, Eu_5Pb_3, and Eu_5Sn_3 are all relatively more stable at these hydrogen loadings and 650 °C.

Structures. The X-ray structures of $Ca_5Sn_3(H_x)$ and Ca_5Sn_3F were refined from single-crystal diffraction data obtained from the products of the high-yield syntheses as well as those of $Eu_5Sn_3H_x$ and Sr_5Pb_3F. The crystallographic parameters for all four studies are given in Table 2, and the results and distances for the calcium phases are reported in Tables 3 and 4. The heavy atom refinements of these gave compositions $Ca_{4.97(2)}Sn_{3.000(3)}(H_x)$ and $Ca_{5.004(6)}Sn_{3.000(2)}F_{0.89(1)}$ with the Ca1 occupancies held at unity. (All of the metal positions were reset to unity in the final refinements.) Interestingly, the largest residual electron density in a Fourier difference map for the hydride was 1.9 e/Å^3 at the center of the tetrahedron where fluoride is bound. This was not refineable with good statistics, but a fixed occupancy gave $B \approx 1.7(8)$. The distance from the fixed position of the interstitial ($\bar{4}2m$) to the surrounding Ca2 tetrahedron is 2.3906(9) Å in the hydride and 2.3972(7) Å in the fluoride, compared with estimated crystal radii sums of 2.24 [38] and 2.33 Å,[39] respectively. Matrix effects that would increase the observed distances are a reasonable cause, judging from Ca2−Ca2 distances in the range 3.6−3.7 Å. The respective Sn2−Sn2 dimer distances of 2.9034(8) and 2.9105(6) Å are appreciably less than the 3.063−3.158 Å values in the more complex semiconducting Zintl phase $Ca_{31}Sn_{20}$ [15] but perhaps for good reasons (below). Other distance differences between the two Ca_5Sn_3Z structures are no more than 0.03 Å.

Table 4. Important Interatomic Distances (Å) in $Ca_5Sn_3(H,F)_x$ (X-ray Data) and in Ca_5Sn_3D (Neutron Data)

atom 1−atom 2	$Ca_5Sn_3H_x$	$Ca_5Sn_3F_{0.9}$	Ca_5Sn_3D
Sn2−Sn2	2.9034(8)	2.9105(6)	2.883(6)
Sn1−Ca1 2×	3.7733(5)	3.7939(5)	3.7676(2)
Sn1−Ca2 8×	3.3941(5)	3.3990(4)	3.396(1)
Sn2−Ca1 2×	3.2154(2)	3.2071(2)	3.219(1)
Sn2−Ca2 2×	3.342(1)	3.3381(8)	3.370(4)
Sn2−Ca2 4×	3.2935(8)	3.2921(6)	3.279(3)
Ca1−Ca2 8×	3.8138(6)	3.8114(5)	3.823(3)
Ca2−Ca2[a]	3.591(2)	3.625(1)	3.599(5)
Ca2−Ca2[b]	3.746(2)	3.732(1)	3.697(6)
Ca2−Ca2[c]	4.575(2)	4.578(2)	
Ca2−Ca2[d] 2×	3.981(2)	4.003(1)	3.941(4)
Ca2−Ca2 4×	4.3157(4)	4.3099(4)	4.326(1)
Ca2−Z	2.3906(9)[e]	2.3972(7)	2.365(3)

[a] Unshared edge of $(A2)_8$. [b] Top of tetrahedron, Figure 2b. [c] Height of trigonal prism along $\bar{c}$. [d] Side edges of tetrahedron. [e] To centroid.

Table 5. Some Neutron Crystallographic Data for Ca_5Sn_3D and CaSn (Impurity Phase)

	Ca_5Sn_3D	CaSn
space group	*I*4/*mcm* (No. 140)	*Cmcm* (No. 63)
a (Å)	8.1453(4)	4.813(1)[a]
b (Å)		11.540(2)
c (Å)	15.0703(8)	4.349(1)
vol (Å^3)	999.8(1)	241.6(1)
density calcd (g/cm^3)	3.710	4.366
refined 2θ region (deg)	10−140	
total no. of points	2424	
weighted fraction (mol %)	79.539(7)	20.461(7)
R_p (%)	5.12	
R_{wp} (%)	6.54	
reduced χ^2	1.871	

[a] Guinier X-ray lattice parameters for CaSn are $a = 4.8121(5)$ Å, $b = 11.544(1)$ Å, $c = 4.3502(4)$ Å, $V = 241.65(5)$ Å^3.

One characteristic in both X-ray diffraction refinements of these structures (and others to follow) is a rather anisotropic displacement parameter only for Ca1, $U_{33}/U_{11} \approx 2.5-3.5$. This is likely just a reflection of the elongated octahedron of tin neighbors about it, ~3.78 Å (×2) to Sn1 plus 3.21 Å (×4) to Sn2 in the dimer. A similar effect has been noted for $Eu_5Ge_3(H_x$[9]), $U_{33}/U_{11} \approx 4.9$, which was concluded to represent a static disorder,[40] and in the related La_5Pb_3O, where La1 could be refined as split atoms 0.33 Å apart.[14]

The presence of hydrogen in this interstitial site was firmly established by a neutron diffraction study of the powdered deuteride (Tables 3 and 5) mixed with the new CaSn (CrB), an impurity at the ~20 mol % level. The distance data are in Table 4. The residuals without inclusion of deuterium in the refinement were unacceptably high (R_p/R_{wp} = 11.07/15.27%), but they became much lower when D was included (5.12/6.54%). The D occupancy was refined to 1.04(2). The calculated fit to the observed neutron diffraction pattern is illustrated in the Supporting Information.

The structure of $Ca_5Sn_3(H,D,F)$, etc. according to the manifold investigations is shown in Figure 1 with the tetragonal axis

(38) Marek, H. S.; Corbett, J. D. *Inorg. Chem.* **1983**, *22*, 3194.
(39) Shannon, R. D. *Acta Crystallogr.* **1976**, *A32*, 751.
(40) Pöttgen, R.; Simon, A. *Z. Anorg. Allg. Chem.* **1996**, *622*, 779.

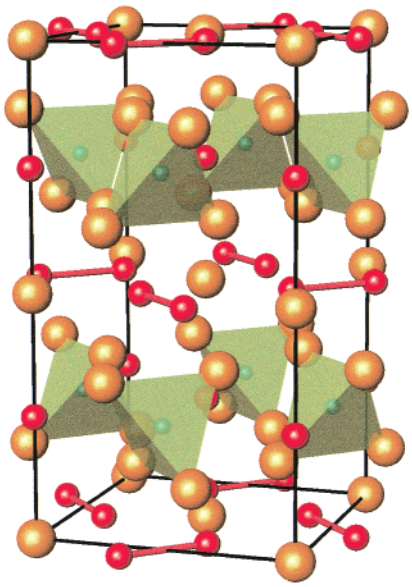

Figure 1. Perspective view off-[100] of the centered tetragonal structure of $Ca_5Sn_3(H,F)$, with $\vec{c}$ vertical. Larger golden and medium red spheres represent Ca and Sn, respectively, and the interstitial H and F are centered in the shaded green tetrahedra. Red bonds mark the characteristic $(Sn2)_2$ dimers.

vertical. The larger gold atoms are calcium, and the medium red ones represent tin. The heavy lines mark the Sn2 dimers, while the necessary H, D, or F atoms center the shaded tetrahedra. A useful description that helps one to understand the structure is in terms of a 1:1 intergrowth between U_3Si_2-like and $CuAl_2$-like slabs,[41] which are shown separately in Figure 2 in [001] sections. The former (top) is centered around $z = 0$, $^1/_2$ (with alternate orientations) and contains the $(Sn2)_2$ dimers inside face-sharing trigonal prisms of calcium together with Ca1-centered cubes of Ca2. The $CuAl_2$-type portion (bottom) at $z = {}^1/_4$, $^3/_4$ contains square antiprisms of Ca2 centered by isolated Sn1 atoms, the former generating the tetrahedral cavities for H, D, F at their interconnections (green). The overall assembly involves alternate sharing of square faces of cubes and antiprisms along 0,0,z and $^1/_2$,$^1/_2$,z (compare with Figure 1), a common feature in other structures as well.[16,20,35]

The structural refinements of $Eu_5Sn_3H_x$ and $Sr_5Pb_3F_x$ were also accomplished from single-crystal X-ray data. The heavy atom composition of the first was previously unreported. The refined atom positions and distances for both are given in Tables 6 and 7. The very similar A2−Z distance within the tetrahedra are now 0.14 and 0.05 larger than the respective sum of six-coordinate crystal radii of A^{2+} and four-coodinate Z^-,[38,39] similar to what was noted above for the two Ca_5Sn_3Z versions. The appreciable $A^{2+}-A^{2+}$ coordination numbers and repulsions are again presumably responsible for the increase. It also seems clear that the Eu−H (centroid) distance is much closer to that for Eu^{2+} rather than Eu^{3+}. The Sn−Sn distance in the former is 0.02−0.03 Å less than that in the $Ca_5Sn_3(H,F)$ phases, whereas the only Pb−Pb dimer distance to compare with the present 3.106(3) Å value seems to be the 3.05(3) Å distance from an old film study of the isotypic $Ba_5Pb_3(H_x)$.[28] The shortest Pb−Pb distance in La_5Pb_3O, where the dimer is judged to be absent, is 3.550(1) Å.[14] A broader treatment of the distances in the stuffed Cr_5B_3-type phases and some interpretations will appear in a forthcoming article.[13]

General Considerations. This article reports on what are seemingly the most egregious of the errors committed or

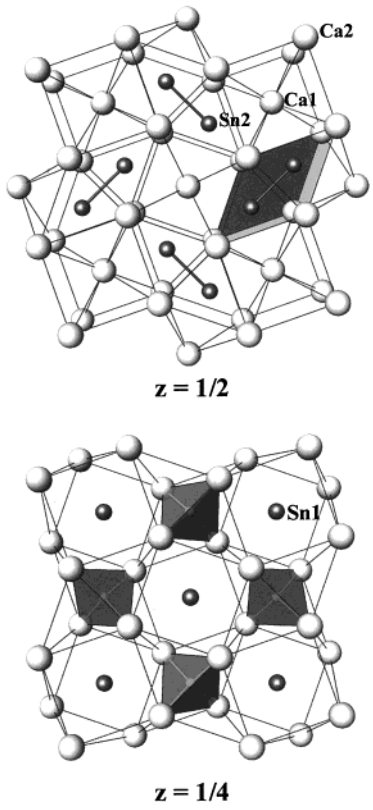

Figure 2. [001] projections of the alternating slabs in the $Ca_5Sn_3(H,F)$ structure (compare Figure 1). Top: The U_3Si_2-like slab centered at $z = 0$, $^1/_2$ (with alternate orientations). Large open and medium solid spheres mark Ca and Sn, respectively, and the highlighted area marks the trigonal prismatic pair of Ca2 that surrounds the dimer. Bottom: $CuAl_2$-like slab centered at $z = {}^1/_4$, $^3/_4$ (with alternate orientations). The tetrahedra about the H or F atoms at 0, $^1/_2$, $^1/_4$, etc. are shaded.

Table 6. Refined Positional Parameters for $Eu_5Sn_3H_x$ and Sr_5Pb_3F

atom	x	y	z	B_{eq} (Å^2)
		$Eu_5Sn_3H_x$		
Eu1	0	0	0	1.81(5)
Eu2	0.16820(7)	$x + {}^1/_2$	0.14967(5)	1.19(3)
Ge1	0	0	$^1/_4$	1.02(5)
Ge2	0.3795(1)	$x + {}^1/_2$	0	0.80(3)
(H	0	$^1/_4$	$^1/_4$)	
		Sr_5Pb_3F		
Sr1	0	0	0	1.6(2)
Sr2	0.1616(2)	$x + {}^1/_2$	0.1504(2)	1.23(6)
Pb1	0	0	$^1/_4$	1.06(6)
Pb2	0.3733(1)	$x + {}^1/_2$	0	0.74(4)
F[a]	0	$^1/_2$	$^1/_4$	1.3(6)

[a] Occupancy is unity.

Table 7. Important Interatomic Distances (Å) in $Eu_5Sn_3H_x$ and Sr_5Pb_3F Structures (A_5Tt_3Z)

atom 1− atom 2	$Eu_5Sn_3H_x$	Sr_5Pb_3F	atom 1− atom 2	$Eu_5Sn_3H_x$	Sr_5Pb_3F
Tt2−Tt2	2.884(3)	3.106(3)	A1−A2 (8×)	3.9190(6)	4.040(2)
Tt1−A1 (2×)	3.8972(3)	3.9895(5)	A2−A2[a]	3.691(2)	3.848(6)
Tt1−A2 (8×)	3.5158(4)	3.619(2)	A2−A2	4.027(2)	3.962(5)
			A2−A2	4.667(2)	4.799(7)
Tt2−A1 (2×)	3.3704(8)	3.4170(6)	A2−A2 (2×)	4.230(2)	4.238(6)
Tt2−A2 (2×)	3.441(2)	3.534(3)	A2−A2 (4×)	4.4530(4)	4.597(1)
Tt2−A2 (4×)	3.403(1)	3.478(3)	A2−Z	2.5497(9)[b]	2.540(3)

[a] Ordered as in Table 4. [b] To centroid.

possible for Cr_5B_3-like phases, those that are uniquely stabilized by hydride (or fluoride). Chloride has not been tried, but the sizes of the cavities in structures of true binaries of this type

(41) Zhao, J.-T.; Corbett, J. D. *J. Alloys Compd.* **1994**, *210*, 1.

would not encourage this prospect, this anion being much better bound in the larger trigonal antiprismatic sites in $MnSi_3$-type hosts, La_5Ge_3Cl, Ca_5Sb_3Cl, and Ba_5Sb_3Cl, for instance.[6,8] (On the other hand, hydride but not fluoride has been incorporated into some Mn_5Si_3-type $(A^{II})_5(Pn)_3Z$.[9]) It is again worthwhile to note that such errors originating from impurity stabilization could probably have been avoided if high-yield syntheses from on-stoichiometry reactions had been a standard expectation. Also, it will be noted that none of the phases described in the present article are silicides or germanides, all of those with Cr_5B_3-based structures occurring both with and without a small interstitial, whereas only one instance with a heavier tetrel, Sr_5Sn_3, falls in the "both" category (below) as far as we know.

For completeness, it is useful to list here the character of the products in other $A^{II}-Tt-H$ systems that will be reported in subsequent articles. Those in which both the Cr_5B_3-type (or Ba_5Si_3-type) binary and a stuffed Ca_5Sn_3F-type (or Ba_5Si_3F-type) ternary hydride phase are stable occur for Ca−Si, Sr−Si, Ba−Si, Eu−Si, Ca−Ge, Sr−Ge, Ba−Ge, Eu−Ge, and Sr−Sn.[13] The majority of the literature on these appears to pertain to the hydride. These more troublesome either/or cases are signaled principally by clear lattice constant changes. However, the rates of change with and the limits of interstitial hydrogen content are generally unknown. Comparisons with lattice constants from the literature can then become more problematic because of uncertainties or variations originating with other factors. Several fluorides and a larger number of X-ray structural studies are also included in this group, and relative hydride−fluoride effects are better considered with these.[13]

A second group have Mn_5Si_3-type binary as well as ternary hydride phases with shifted lattice constants for the latter, namely, Sm−Si, Sm−Ge, Sm−Sn, Sm−Pb, Yb−Si, Yb−Ge, and Yb−Pb. (But the Yb−Ge system lacks the Mn_5Si_3-type binary.) Most of the data in the literature are again probably those of the hydrides. It will be noted that this group presumably involves at least some trivalent cations as well because of the greater electronic requirements of the characteristically isolated anions in both the Mn_5Si_3 structure and its stuffed version, presuming of course that octet configurations still apply to the anions (and this is also a question).[9] Finally, the Ca−Pb and Yb−Pb systems involve complex and incompletely understood $A_{5+x}Pb_3$ superstructures evidently related to an Mn_5Si_3 parent, plus the new $Yb_{31}Pb_{20}$ compound in the latter ($a = 12.5270(8)$ Å, $c = 40.453(4)$ Å), and hydrogen may be incorporated in the former as well.[42,43] No Cr_5B_3-like examples have been found in these Ca−Pb or Yb−Pb systems. Also, we were unable to gain the reported Mn_5Si_3 (substructure) form of Yb_5Pb_3[44] except when the sample was quenched from 825 to 900 °C rather than cooled at 10−12 °C/h.

We have also explored some electron-poorer $(A^{II})_5Tr_3$ systems for the Ga, In, Tl triels, confirming that reported Cr_5B_3-type binaries Ca_5Ga_3 and Sr_5In_3 as well as the new Sm_5Ga_3 are not hydrides but that the thallide is, $Sr_5Tl_3H_{\sim 1}$. These systems will also be reported separately.[9] The distances in the Tr_2 dimers are of interest with respect to their bonding configurations.

Properties and Bonding. In this connection, understanding more about these compounds and their properties needs to start with the recognition that the structural classification of the $(A^{II})_5Tt(Tt_2)$ compounds as electron-precise Zintl phases is in fact not correct in the sense that at least some, and perhaps all, are metallic. Starting from this point, the oxidation of A_5Tt_3 phases to hydride or fluoride derivatives is not so unusual or problematic. A good deal more magnetic susceptibility as well as some resistivity data in support of these conclusions are available for those compounds that have Cr_5B_3-type structures for both binary and ternary (stuffed) products.[13] For example, Ca_5Ge_3 and Ca_5Ge_3H have Pauli-like magnetic susceptibilities and metal-like resistivities of ∼50 and ∼130 $\mu\Omega$ cm, respectively, at 290 K. Magnetic properties of a few of the oxidized products described herein have also been measured and also found to exhibit Pauli-like susceptibilities. Figure 3 shows susceptibility data for $Ca_5Sn_3H_x$ and $Ca_5Sn_3F_{0.9}$, while Sr_5Pb_3F gives very similar results, χ_{mol} decreasing slowly from 5.8 to 3.5 ($\times 10^{-4}$ emu mol^{-1}) between 6 and 300 K.

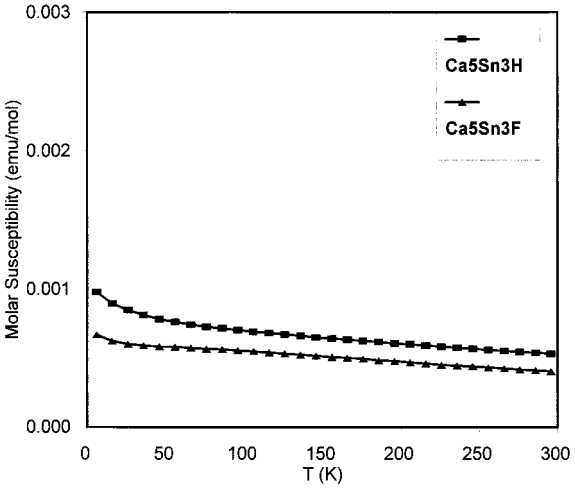

Figure 3. Molar magnetic susceptibilities of $Ca_5Sn_3H_x$ and $Ca_3SnF_{0.9}$ as a function of temperature at 3 T.

From a more general viewpoint, the oxidation leading to these products would be expected to deplete the highest-lying and nominally filled π^*[4] levels of an ideal isolated Sn_2^{-6}, etc. if such an assignment were valid. The effect is reflected in the extended Hückel band calculation results for Ca_5Sn_3H shown in Figure 4, where the Fermi level falls in the upper reaches of the π^* band (see the Sn2−Sn2 COOP curve). However, this calculation used default valence energy values for the atoms, and the large gap obtained is not very realistic in terms of the evident metallic character of Ca_5Sn_3H. In other words, some π^* electrons must have spilled over into the conduction band. Furthermore, as will be detailed later, the Tt2−Tt2 (and Tr2−Tr2) bond lengths in the dimers in general do appear to *shorten* as π^* electrons are removed, although matrix effects from the lattice may complicate this issue.[9,43]

For the moment, interpretation of the present Sn−Sn distances, 2.88−2.91 Å, is somewhat complex because they appear to be influenced by three different electronic factors. First, the loss of a single π^* electron from the oxidation by H or F is the simplest. This would produce a net Sn−Sn bond order of 1.5 in an isolated species if we lump σ and π bonding together, as is commonly done with, and is better justified for, lighter main-group elements. A second factor, which also would formally enhance the Sn−Sn bonding, is further delocalization of some π^* electron density, as reflected in the Pauli-like paramagnetism observed for the ternary samples. Third is the effect of "charge repulsion" in the dimers that serves to lengthen the bonds,[45] in opposition to the other effects. The first two appear to be real

(42) Guloy, A. M. Ph.D. Dissertation, Iowa State University, Ames, IA, 1992.
(43) Leon-Escamilla, E. A. Ph.D. Dissertation, Iowa State University, Ames, IA, 1996.
(44) McMasters, D. T.; Gschneidner, K. A., Jr. *Trans. Metall. Soc. AIME* **1967**, *239*, 781.
(45) Nesper, R. *Prog. Solid State Chem.* **1990**, *20*, 1.

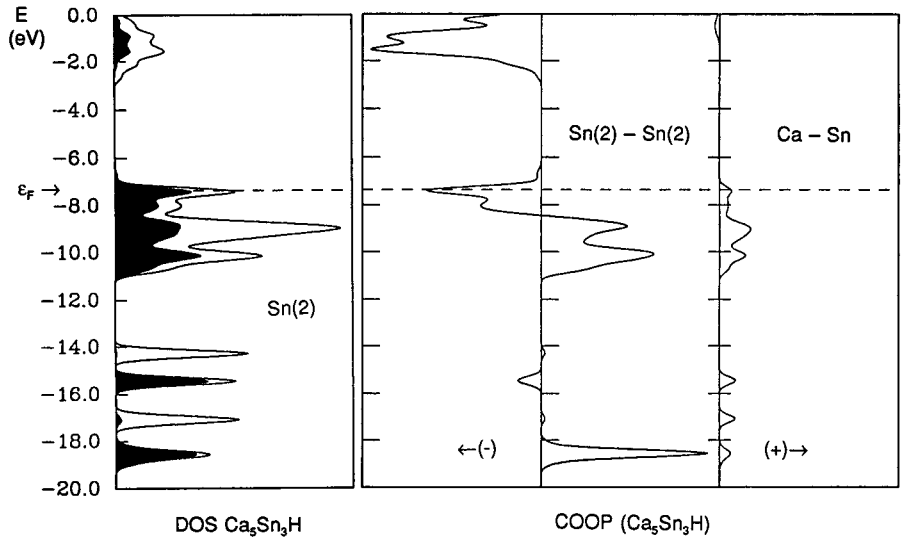

Figure 4. Results of extended Hückel band calculations for Ca_5Sn_3H: (left) total DOS (density of states) with the Sn2 contributions projected out; (right) COOP (crystal orbital overlap population) curves for Sn2−Sn2 (dimer) and total Ca−Sn interactions.

when the 2.88−2.91 Å distances here are compared with those in a classical Zintl phase, 3.06−3.16 Å in the dimers in semiconducting $Ca_{31}Sn_{20}$ and very similar values in the linear formal Sn_5^{12-} anion in which charge repulsion should be less.[16] The similar (but poorly metallic) $Yb_{36}Sn_{23}$ exhibits very comparable distances, 3.10−3.16 Å in the dimers and 3.02−3.11 Å within the hexameric Sn_6^{14-}.[34] On the other hand, the absence of both charge repulsion and strong Coulombic effects in general gives still shorter Sn−Sn (single bond) distances: 2.84 Å in gray tin, 2.82−2.86 Å in K_8Sn_{25}, where the 3b-Sn^- atoms are isolated, and 2.81−2.87 Å in the defect chlathrate-I structure of Rb_8Sn_{44} when distances to those defect positions are omitted.[46] Thus, a set of consistent effects can be envisioned if the comparisons are limited just to those among similar compounds. This becomes increasingly important and evident among the triels and presumably even more so for the "diels", the increased absence of formal π^* bonding electrons perhaps being major factors in the stability of these unusual compounds.

Note Added in Proof. An evident hydride of Ca_5Sn_3 has recently been reported: Palenzona, A.; Manfrinetti, P.; Fornasini, M. L. *J. Alloys Compd.* **2000**, *312*, 165.

Acknowledgment. We thank P. Dervengas and C. Stassis for the neutron diffraction data and refinements, and we thank J. Ostenson for the magnetic susceptibility measurements. All are affiliated with the Condensed Matter Physics Program, Ames Laboratory, DOE.[1]

Supporting Information Available: Tables of additional X-ray crystallographic data, positional and anisotropic displacement parameters for four X-ray structures, and crystallographic data and a plot of the results for the neutron diffraction study. This material is available free of charge via the Internet at http://pubs.acs.org.

IC0010306

(46) Zhao, J.-T.; Corbett, J. D. *Inorg. Chem.* **1994**, *33*, 5721.